

Simulation of Diffuse Optical Tomography using COMSOL Multiphysics®

S.A.M. Kirmani^{*1}, L. Velmanickam¹, D. Nawarathna¹, S.S. Sherif², and I.T. Lima Jr.¹

¹Department of Electrical and Computer Engineering, North Dakota State University, Fargo, ND, USA

²Department of Electrical and Computer Engineering, University of Manitoba, Winnipeg, MB, Canada

*Corresponding author: syedabdulmannan.kirm@ndsu.edu

Abstract: We show that the COMSOL Multiphysics® can efficiently simulate the diffusion equation (DE) in diffusive optical tomography systems. Using our implementation, we simulate a frequency domain diffusive optical tomography system two order of magnitude faster than the standard Monte Carlo method of light transport in tissues. This model can be used in the design and optimization of diffusive optical tomography systems for biomedical applications.

Keywords: Diffuse Optical Tomography, Diffuse Photon Density Waves

1. Introduction

In addition to analyzing medical history and conducting physical examination of patients, physicians perform various medical diagnostic procedures for proper diagnosis of medical conditions. These diagnostic procedures include several imaging techniques, such as X-ray radiography, computed tomography (CT-scan), magnetic resonance imaging (MRI). Many of these techniques employ X-rays, or other electromagnetic radiation, that have harmful effects on the human body. For example, X-rays are classified as carcinogen, since they can cause mutations in human DNA and might lead to cancer later in life. However, their utility to provide essential information for medical diagnosis justifies their use for imaging. Optical tomography techniques are quite popular because they employ infrared light, which is non-ionizing for biological tissues and, thus, lacks the harmful effects of X-rays and other ionizing radiation.

Biological tissues are considered as turbid media in which light penetrates to a certain depth before being absorbed or scattered. This diffusion of light in a tissue provides an opportunity to non-invasively probing and imaging up to a certain depth. Generally, light absorption is much weaker than light scattering in most biological tissues. The mean free path between photon scattering events is on the order of 0.1 mm, whereas the

mean absorption length can extend to 10 – 100 mm [1]. Therefore, light scattering is the dominant physical phenomenon when dealing with propagation of light in biological tissues.

We may classify optical tomography techniques into two main groups: (a) techniques based on spatial coherence of light, such as optical coherence tomography (OCT) and confocal microscopy (b) and techniques based on diffusive propagation of light in a tissue, such as diffusive optical tomography (DOT) and DPDW methods [2]. The techniques based on diffuse propagation of light in a tissue can be further classified into three main categories based on the type of light source used in the process. These techniques are summarized in table 1.

Table 1: Techniques based on diffusive propagation of light in a tissue

Light Source	Diffuse Optical Technique
Continuous Wave Light Source	Continuous Wave (CW) methods
Intensity Modulated Light Source	Frequency Domain (FD) methods
Time pulsed Light Source	Time Domain (TD) methods

Our work involves DPDW that is a frequency domain diffuse optical tomography technique employing intensity modulated light sources.

The ability of DPDW to determine the optical properties of tissues is critical for many biomedical applications. It is employed to observe and analyze cutaneous and subcutaneous tissue damage. This imaging technique is a useful aid for the diagnosis and treatment of pressure ulcers, skin and tissue injuries, wounds and burns.

2. Solving the Diffusion Equation using COMSOL Multiphysics®

The operating principle of any optical tomography technique is the result of the interaction of light with a biological tissue. Biological tissues are turbid media, in which light propagation and light-tissue interaction are modeled analytically by the radiative transfer equation (RTE), and can be numerically solved using Monte Carlo (MC) simulations [1-4]. Since the RTE is numerically costly to solve, it is often approximated by the diffusion equation (DE). In this work we use the Helmholtz Equation model in COMSOL Multiphysics® to solve the DE.

3. Theory

The main physical quantity in RTE is the light radiance $L(\vec{r}, \hat{s}, t)$ ($\text{W cm}^{-2} \text{sr}^{-1}$) which is defined as the *light power per unit of area travelling in the \hat{s} direction at position \vec{r} and time t* [3].

The RTE is derived from the principle of conservation of energy and governs light radiance in an infinitesimal volume element [1, 4]:

$$\frac{1}{v} \frac{\partial L(\vec{r}, \hat{s}, t)}{\partial t} = -\hat{s} \cdot \nabla L(\vec{r}, \hat{s}, t) - \mu_t L(\vec{r}, \hat{s}, t) + \mu_s \int_{4\pi} L(\vec{r}, \hat{s}', t) p(\hat{s}, \hat{s}') d\hat{s}' + S(\vec{r}, \hat{s}, t). \quad (1)$$

The left hand side of (1) represents the change in radiance in the infinitesimal volume element at position \vec{r} and time t in an \hat{s} direction. The right hand side of (1) has all the terms that contribute to that change through either gain or loss. For time independent or steady state responses, the left hand side of (1) is zero. The term $\hat{s} \cdot \nabla L(\vec{r}, \hat{s}, t)$ accounts for the loss of light radiance in the infinitesimal volume element at position \vec{r} and time t in the \hat{s} direction due to divergence. The losses due to absorption and scattering are accounted for in $\mu_t L(\vec{r}, \hat{s}, t)$. It depends on the extinction coefficient, $\mu_t = \mu_a + \mu_s$ where μ_a (cm^{-1}) is the absorption coefficient and μ_s (cm^{-1}) is the scattering coefficient of light. The phase function $p(\hat{s}, \hat{s}')$ gives the probability that light with incident propagation direction \hat{s} will be scattered into the \hat{s}' direction. Generally, the phase function depends only on the direction between the scattered and the incident directions, that is $p(\hat{s}, \hat{s}') = p(\hat{s} \cdot \hat{s}')$. The anisotropy factor, g , is defined from the phase function as $g \equiv \int_{4\pi} p(\hat{s} \cdot \hat{s}') (\hat{s} \cdot \hat{s}') ds = g(\cos \theta)$. Typically for

biological tissues, g is close to 1. The term $\mu_s \int_{4\pi} L(\vec{r}, \hat{s}', t) p(\hat{s}, \hat{s}') d\hat{s}'$ provides the gain in light radiance in the infinitesimal volume element at position \vec{r} and time t in the \hat{s} direction due to scattering of light from adjacent volumes. v is the speed of light in the medium. $S(\vec{r}, \hat{s}, t)$ ($\text{W cm}^{-3} \text{sr}^{-1}$) is the power per unit volume emitted by sources at position \vec{r} and time t in the \hat{s} direction.

The RTE is difficult to solve analytically, since it has six independent variables (x, y, z, θ, ϕ, t). The P_1 Approximation for light radiance, given by (2) is employed to reduce its complexity which is valid when radiance is nearly isotropic that is the case in high albedo, $a = \frac{\mu_s}{\mu_a + \mu_s}$, scattering mediums like biological tissues. In such mediums, photon absorption length $l_a = 1/\mu_a$ is much larger than the photon scattering length $l_s = 1/\mu_s$. So light radiances diffuse into the tissue to a certain depth before being absorbed. Hence, the P_1 approximation given by (2) is also known as the diffusion approximation [3]:

$$L(\vec{r}, \hat{s}, t) = \frac{1}{4\pi} \varphi(\vec{r}, t) + \frac{3}{4\pi} J(\vec{r}, t) \cdot \hat{s}. \quad (2)$$

In (2), the photon fluence rate $\varphi(\vec{r}, t)$ (W cm^{-2}) is defined as the *total power per unit area moving radially outward from the infinitesimal volume element at position \vec{r} and time t* [3]:

$$\varphi(\vec{r}, t) \equiv \int_{4\pi} L(\vec{r}, \hat{s}, t) ds. \quad (3)$$

Similarly, the photon flux $J(\vec{r}, t)$ (W cm^{-2}) is defined as the *power per unit area travelling in the \hat{s} direction at position \vec{r} and time t* [3]:

$$J(\vec{r}, t) \equiv \int_{4\pi} L(\vec{r}, \hat{s}, t) \hat{s} ds. \quad (4)$$

If we integrate the RTE, equation (1), over all solid angles, we get a continuity equation relating photon fluence rate and the photon flux [3]:

$$\frac{1}{v} \frac{\partial \varphi(\vec{r}, t)}{\partial t} + \nabla \cdot J(\vec{r}, t) + \mu_a \varphi(\vec{r}, t) = S(\vec{r}, t), \quad (5)$$

where $S(\vec{r}, t)$ (W cm^{-3}) is the *total power per unit volume emitted radially outward from position \vec{r} and time t* [3]:

$$S(\vec{r}, t) \equiv \int_{4\pi} Q(\vec{r}, \hat{s}, t) \hat{s} ds. \quad (6)$$

We substitute equation (2) into equation (1) and multiply the resulting equation by \hat{s} and integrate over all solid angles to get another relation between photon fluence rate and photon flux [3]:

$$\nabla \varphi(\vec{r}, t) = -\frac{3}{v} \frac{\partial J(\vec{r}, t)}{\partial t} - 3\mu_t J(\vec{r}, t) + 3 \int Q(\vec{r}, \hat{s}, t) \hat{s} ds + 3\mu_s g J(\vec{r}, t). \quad (7)$$

Assuming isotropic sources, $Q(\vec{r}, \hat{s}, t) = Q(\vec{r}, t)$, the integral over Q in equation (7) is zero. Moreover, if we assume slow temporal variations in photon flux then time derivative of photon flux is negligible compared to the rest of the terms on the right hand side of the equation (7). With these assumptions we obtain at Fick's law of diffusion [3]:

$$\nabla\varphi(\vec{r}, t) = -3(\mu'_s + \mu_a)J(\vec{r}, t), \quad (8)$$

where $\mu'_s \equiv (1 - g)\mu_s$ is defined as the reduced scattering coefficient.

Finally we get the DE for the photon fluence rate by substituting equation (8) into equation (5) [1-3]:

$$-\nabla \cdot (D(\vec{r})\nabla\varphi(\vec{r}, t)) + \mu_a(\vec{r})\varphi(\vec{r}, t) + \frac{1}{v}\frac{\partial\varphi(\vec{r}, t)}{\partial t} = S(\vec{r}, t), \quad (9)$$

where $D(\vec{r})$ is the photon diffusion coefficient defined as $D(\vec{r}) \equiv \frac{1}{3(\mu'_s(\vec{r}) + \mu_a(\vec{r}))}$.

Intensity modulated light sources generate fluence rate disturbances that behave as overdamped waves which are termed as DPDW. In equation (9), if we assume the source term has dc and ac parts and can be written in the form $S(\vec{r}, t) = S_{dc}(\vec{r}) + S_{ac}(\vec{r})e^{-i\omega t}$. Then the DPDW solutions are those that oscillate at the same angular frequency as the source and have the following general form [1-3]:

$$\varphi_{ac}(\vec{r}, t) = U(\vec{r})e^{-i\omega t}, \quad (10)$$

Substituting value of $\varphi_{ac}(\vec{r}, t)$ in equation (9), we have

$$-\nabla \cdot (D(\vec{r})\nabla U(\vec{r})e^{-i\omega t}) + \mu_a(\vec{r})U(\vec{r})e^{-i\omega t} + \frac{1}{v}\frac{\partial U(\vec{r})e^{-i\omega t}}{\partial t} = S_{ac}(\vec{r})e^{-i\omega t}. \quad (11)$$

After simplification of equation (11), we have

$$-\nabla \cdot (D(\vec{r})\nabla U(\vec{r})) + \left(\mu_a(\vec{r}) - \frac{i\omega}{v}\right)U(\vec{r}) = S_{ac}(\vec{r}). \quad (12)$$

Equation (12) is the required Helmholtz equation that was solved in COMSOL to obtain DPDW.

The propagation of photons through a medium can be modeled by random walks. Each photon is assumed to travel in a straight line until an interaction with the medium particles occur. These interactions result in either scattering, random change in propagation direction, or absorption of the photon. The average length of the photon's straight line random walk steps

between these interactions is termed as transport mean free path $l_{tr} = 1/(\mu'_s + \mu_a)$.

The validity of the DE for photon fluence rate (equation (9)) depends on the following assumptions [3]:

- P_1 approximation of RTE (equation (2)) is valid that is light radiance is nearly isotropic ($\varphi(\vec{r}, t) \gg |J(\vec{r}, t)|$)
 - The isotropy condition is satisfied when $\mu'_s \gg \mu_a$, and when photon propagation distances are large as compared to l_{tr} .
 - Rule of thumb: μ'_s/μ_a should exceed 10.
- Source Isotropy, $Q(\vec{r}, \hat{s}, t) = Q(\vec{r}, t)$
- Slow temporal flux variations, $\frac{1}{v}\frac{\partial J(\vec{r}, t)}{\partial t} \ll (\mu_t - \mu_s g)J(\vec{r}, t)$
- Rotational Symmetry, $p(\hat{s}, \hat{s}') = p(\hat{s} \cdot \hat{s}')$

The radiance is no longer isotropic near a boundary such as an air-tissue interface. In that case the DE needs to be modified to account for the Fresnel reflections at the interface. Usually, photons escaping the tissue do not come back, therefore, the incoming irradiance J_{in} near the boundary is due to the Fresnel reflections of radiance that was moving out towards the boundary.

The incoming irradiance J_{in} is defined as the total light power per unit area travelling into the diffuse medium at the boundary [3]:

$$J_{in} \equiv \begin{cases} \int_{\hat{s} \cdot \hat{n} < 0} L(\hat{s})\hat{s} \cdot (-\hat{n})ds \\ \int_{\hat{s} \cdot \hat{n} > 0} R_{Fresnel}(\hat{s})L(\hat{s})\hat{s} \cdot (\hat{n})ds \end{cases}, \quad (10)$$

where $R_{Fresnel}(\hat{s})$ is the Fresnel reflection coefficient for light incident upon the boundary in a direction \hat{s} from within the medium.

The partial flux boundary condition (also known as Robin boundary condition) that relates the fluence rate to its gradient at the boundary is calculated by substituting the value of radiance from the P_1 approximation in equation (2) and an appropriate form of Fresnel reflection coefficient in equation (10) [3]:

$$\varphi = z_b \hat{n} \cdot \nabla\varphi. \quad (11)$$

Equation (11) gives the fluence rate on the boundary. Here, the unit vector \hat{n} points from inside the tissue to outside as shown in Fig. 1 and z_b is the z-coordinate of the boundary [3]:

$$z_b = \frac{2l_{tr}(1 + R_{eff})}{3(1 - R_{eff})}, \quad (12)$$

where R_{eff} is the effective reflection coefficient which accounts for the index mismatch between the diffusing medium and the air that is given by [3 - 5]:

$$R_{eff} \approx -1.440n^{-2} + 0.710n^{-1} + 0.668 + 0.0636n, \quad (13)$$

where n is the ratio of the index of refraction inside and outside the diffusing medium [3 - 5]:

$$n = \frac{n_{in}}{n_{out}}, \quad (14)$$

The value of R_{eff} in equation (13) was approximated by Egan and Hilgeman [3-6] and is valid for $1.0 < n < 2.2$.

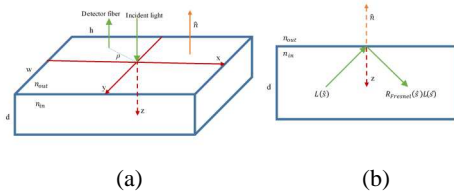


Figure 1. (a) Geometrical model of the tissue (b) Tissue cross-section.

In this work, we considered a geometrical model of the tissue as in Fig. 1. The w , h and d were large compared to the wavelength of the incident light. The geometrical model considered has azimuthal symmetry about the z -axis such that the photon fluence rate only depends on the radial and axial cylindrical coordinates ρ and z .

4. Results and Discussion

We obtained DPDW phase (Figure 2) and intensity attenuation (Figure 3) at a wide range of source - detector separation distances. In Figure 2 plot (a) is obtained for 0.5% and plot (b) is obtained for 2% concentration of intralipid - water solution. Figure 3 is plotted for 0.5% concentration of intralipid - water solution. The refractive indices of water and intralipid are 1.33 and 1.47 respectively. In Figure 2 plot (a) we have $\mu_s = 5.5 \text{ cm}^{-1}$, $g = 0.8$, $\mu_a = 0.01 \text{ cm}^{-1}$, in plot (b) we have $\mu_s = 22 \text{ cm}^{-1}$, $g = 0.8$, $\mu_a = 0.01 \text{ cm}^{-1}$. The modulation frequency is 100 MHz and the wavelength of incident light is 685 nm for readings in Figure 2. For figure 3, modulation frequency is 200 MHz and

wavelength of the incident light is 685 nm. $\mu_s = 5.5 \text{ cm}^{-1}$, $g = 0.8$, $\mu_a = 0.01 \text{ cm}^{-1}$ for the results in Figure 3.

To achieve a similar accuracy of the COMSOL simulation of the DPDW, we needed to use 100 times more computer time in the Monte Carlo method. Our results are in agreement with Monte Carlo simulations and experimental results shown in [8].

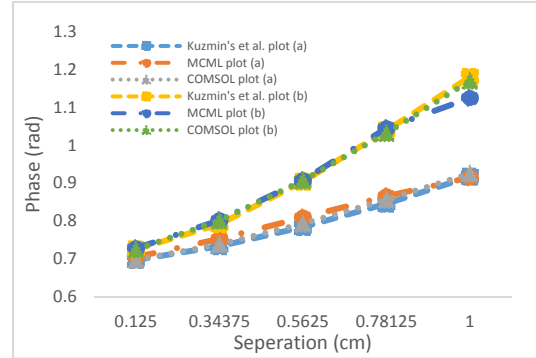


Figure 2. DPDW phase against source - detector separations for two different concentrations of aqueous intralipid solution

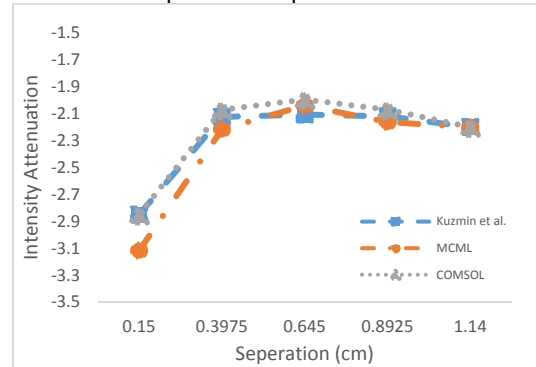


Figure 3. DPDW intensity attenuation against source - detector separation

5. Conclusions

Our simulations of a diffusive optical tomography system based on COMSOL Multiphysics® produce accurate results two orders of magnitude faster than the standard Monte Carlo method of light transport in tissues. Therefore, COMSOL is a practical tool in the simulation of DPDW in optical tomography systems for biomedical applications, such as the diagnosis of cutaneous and subcutaneous skin damage.

6. References

1. L. V. Wang and H. Wu, *Biomedical Optics: Principles and Imaging*, Wiley, 2012
2. L. O. Svaasand, T. Spott, J. B. Fishkin, T. Pham, B. J. Tromberg and M. W. Berns, Reflectance measurements of layered media with diffuse photon-density waves: a potential tool for evaluating deep burns and subcutaneous lesions, *Physics in Medicine and Biology*, **44**(3), 801-813 (1999)
3. T. Durduran, R. Choe, W. B. Baker, & A. G. Yodh, Diffuse optics for tissue monitoring and tomography, *Reports on Progress in Physics*, **73**(7), 076701 (2010)
4. S. L. Jacques, & B. W. Pogue, Tutorial on diffuse light transport, *Journal of Biomedical Optics*, **13**(4), 041302 (2008)
5. M. Schweiger, S. R. Arridge, M. Hiraoka, & D. T. Delpy, The finite element method for the propagation of light in scattering media: Boundary and source conditions, *Medical Physics*, **22**(11), 1779 – 1792 (1995)
6. W. G. Egan and T. W. Hilgeman, *Optical properties of inhomogeneous materials: applications to geology, astronomy, chemistry and engineering*, Academic Press, 1979.
7. L. Wang, S. L. Jacques, & L. Zheng, MCML— Monte Carlo modeling of light transport in multi-layered tissues, *Computer Methods and Programs in Biomedicine*, **47**(2), 131 – 146 (1995)
8. V. L. Kuzmin, M. T. Neidrauer, D. Diaz, L. A. Zubkov, Diffuse photon density wave measurements and Monte Carlo simulations, *Journal of Biomedical Optics*, **20**(10), 105006 (2015)